

An Updated Experimental Evaluation of Graph Bipartization Methods

TIMOTHY D. GOODRICH, North Carolina State University, USA

ERIC HORTON, North Carolina State University, USA

BLAIR D. SULLIVAN, North Carolina State University, USA and University of Utah, USA

We experimentally evaluate the practical state-of-the-art in graph bipartization (ODD CYCLE TRANSVERSAL), motivated by recent advances in near-term quantum computing hardware and the related embedding problems. We assemble a preprocessing suite of fast input reduction routines from the ODD CYCLE TRANSVERSAL (OCT) and VERTEX COVER (VC) literature, and compare algorithm implementations using QUADRATIC UNCONSTRAINED BINARY OPTIMIZATION problems from the quantum literature. We also generate a corpus of frustrated cluster loop graphs, which have previously been used to benchmark quantum annealing hardware. The diversity of these graphs leads to harder OCT instances than in existing benchmarks.

In addition to combinatorial branching algorithms for solving OCT directly, we study various reformulations into other NP-hard problems such as VC and INTEGER LINEAR PROGRAMMING (ILP), enabling the use of solvers such as CPLEX. We find that for heuristic solutions with time constraints under a second, iterative compression routines jump-started with a heuristic solution perform best, after which point using a highly tuned solver like CPLEX is worthwhile. Results on exact solvers are split between using ILP formulations on CPLEX and solving VC formulations with a branch-and-reduce solver. We extend our results with a large corpus of synthetic graphs, establishing robustness and potential to generalize to other domain data. In total, over 8000 graph instances are evaluated, compared to the previous canonical corpus of 100 graphs.

Finally, we provide all code and data in an open source suite, including a Python API for accessing reduction routines and branching algorithms, along with scripts for fully replicating our results.

CCS Concepts: • **Mathematics of computing** → *Combinatorial optimization*.

Additional Key Words and Phrases: Odd cycle transversal, near-term quantum computing, vertex cover, integer linear programming

1 INTRODUCTION

ODD CYCLE TRANSVERSAL (OCT), the problem of deleting vertices to make a graph bipartite, has been well-studied in the theory community over the last two decades. Techniques such as *iterative compression* [Hüffner 2009; Reed et al. 2004] and *branch-and-reduce* [Akiba and Iwata 2016; Lokshтанov et al. 2014] have led to significant improvements in both worst-case and experimental run times. These improvements are most drastically seen on the canonical OCT benchmark, Wernicke’s MINIMUM SITE REMOVAL dataset [Wernicke 2003] (denoted WH), where run times have dropped from over 10 hours [Wernicke 2003] to under 3 minutes [Hüffner 2009] to under 1 second per instance for multiple state-of-the-art solvers [Akiba and Iwata 2016]. While these results illustrate the rapid algorithmic advances, they also show that new data is needed for further study.

Recently, a need for practical graph bipartization algorithms has arisen in quantum computing, where the hardware and/or problem structure may naturally have underlying bipartite structure that can be exploited algorithmically¹. In contrast to the WH data – which was expected to be bipartite barring read errors – problem instances from quantum annealing may not be close to bipartite. Additionally, in the quantum setting “good enough” solutions are of interest since OCT may be solved as a subroutine in a larger automated compiler. This introduces a run time vs. solution quality trade-off previously not considered. In this work, we combine richer data with various timeout scenarios in order to provide a modernized evaluation of OCT methods.

1.1 Related Work

Modern theoretical advances on OCT began with the seminal result of Reed, Smith, and Vetta [Reed et al. 2004], who showed that the problem – which asks one to remove the minimum number of vertices k to produce a bipartite subgraph – is fixed-parameter tractable with parameter k using the technique of *iterative compression*. This algorithm was initially shown to run in time $O(4^k km)$, but improved analyses showed a $O(3^k km)$ run time and simpler algorithms for the compression routines [Hüffner 2009; Lokshтанov et al. 2009]. The next theoretical improvement came from an improved algorithm and analysis for VERTEX COVER (VC) and a (straightforward) conversion of an OCT instance to a VC instance. This strategy results in an $O^*(2.3146^{k'})$ algorithm,² where k' denotes the gap between an optimal solution to VERTEX COVER and the solution given by the linear programming (LP) relaxation [Lokshтанov et al. 2014]. Recent work has used the half-integrality of LP-relaxations to reduce the polynomial in n at the cost of a higher parameterized term, resulting in an $O(4^k n)$ algorithm for OCT [Iwata et al. 2014], and $O^*(4^k)$ [Wahlström 2017] and $O(4^k n)$ [Iwata et al. 2017] algorithms for the more general problem of NON-MONOTONIC CYCLE TRANSVERSAL. Other algorithmic results for OCT include a $O(\log \sqrt{n})$ -approximation algorithm [Agarwal et al. 2005], a randomized algorithm based on matroids [Kratsch and Wahlström 2014], and a subexponential algorithm on planar graphs [Lokshтанov et al. 2012].

On the practical side, the first implementation was a branch-and-bound algorithm by Wernicke in 2003 [Wernicke 2003] used for studying single nucleotide polymorphisms. A greedy depth-first search heuristic was used to identify upper bounds on OCT, and several sparse graph reduction routines were applied before branching. A Java implementation of this algorithm solved most WH instances within a 10 hour timeout. In 2009, Hüffner implemented a refined iterative compression algorithm [Hüffner 2009] with additional pruning for infeasible assignments and symmetry in the compression routine’s branching algorithm to achieve experimentally faster run times; all of the WH instances could then be solved within three minutes. Hüffner compared this algorithm against an ILP formulation using the GNU Linear Programming Kit (GLPK) [GNU 2017], which had unfavorable run times. More recently, Akiba and Iwata [Akiba

¹For example, the D-Wave Chimera hardware is bipartite, and upcoming Pegasus hardware admits a large complete bipartite graph embedding.

² $O^*(f(k))$ denotes $O(f(k)n^c)$ for some constant c

and Iwata 2016] used a VC-solver based on branch-and-reduce to solve OCT using a standard transformation to VC [Lokshtanov et al. 2014]. The authors reported that their open source Java implementation could solve all WH data within a second, while competing implementations based on maximum clique and an ILP formulation solved using CPLEX [IBM 2017] all finished within three seconds.

1.2 Our Contributions

In this work, we collect existing OCT techniques, provide a common Python API for running these algorithms, and evaluate them within a broader experimental envelope, incorporating quantum-inspired data and use cases. We also provide a frame for generalizing our conclusions with a large synthetic corpus representing a variety of random graph models.

Whereas OCT can be computed within seconds for all graphs in the previous WH dataset [Hüffner 2009; Wernicke 2003], we provide a new, significantly more difficult benchmark corpus. Motivated by the widespread usage of QUADRATIC UNCONSTRAINED BINARY OPTIMIZATION (QUBO) problems in quantum annealing research [Neven et al. 2008], we select QUBO instances from a recent survey [Dunning et al. 2015] that would be of interest to practitioners working on near-term quantum annealers. These datasets are selections from Glover, Kochenberger, and Alidaee [Glover et al. 1998] (denoted GKA) and Beasley [Beasley 1998] (denoted Beas1ey). Not only do these datasets contain significantly harder OCT instances, they also represent a wider array of graph properties such as number of vertices, edge density, degree distribution, etc., than the WH benchmark.

Collecting previous code and providing missing implementations, we assemble a unified Python API allowing easy comparison of prior work. Preprocessing routines are taken from the OCT [Wernicke 2003] and VC literature [Akiba and Iwata 2016] and applied to all datasets to harden the benchmark corpus. Heuristics for OCT upper bounds [Goodrich et al. 2018b; Wernicke 2003] are collected and implemented as a standalone heuristic ensemble solver for stochastically sampling ‘good enough’ solutions. We use these heuristic solutions, along with a density-first heuristic for the compression ordering, to jump-start the iterative compression algorithm of Hüffner [Hüffner 2009]. These combinatorial algorithms for solving OCT directly are complemented by VC-based [Akiba and Iwata 2016] and ILP-based [IBM 2017] solvers.

In quantum-specific experiments, we examine two distinct use cases. First, to represent scenarios where an automated compiler may use OCT as a subroutine and accept heuristic solutions, we evaluate the heuristic ensemble, iterative compression, and the ILP formulation under timeouts of 0.01, 0.1, 1, and 10 seconds. We find that the iterative compression implementation jump-started with heuristic solutions performs best for timeouts less than a second, after which it is worth paying the overhead of using an ILP solver such as CPLEX. In a second use case where an exact solution is required in order to recognize un-embeddable quantum programs, we evaluate iterative compression, VC-based, and ILP-based exact solvers. Here we again find that ILP formulations solved by CPLEX dominate, typically by at least an order of magnitude.

Generalizing these results, we generate synthetic graphs using four random graph generators – including the frustrated cluster loop model, which has been previously used to generate instances for quantum annealing – and evaluate whether “generic” instances matching the density, degree distribution, etc. exhibit similar effectiveness of reduction routines and solver run times. We find that our results on QUBO data are robust, with the same best practice recommendations. This experimental evidence provides practitioners with a useful reference for developing custom solutions for particular applications.

Our work is fully replicable, with documented code [Goodrich et al. 2018a] open sourced under the BSD 3-Clause license. For the interested reader, Appendix A contains implementation details and Appendix B contains extended results.

2 BACKGROUND

We denote a graph $G = (V, E)$. For a set of vertices S , we denote the subgraph induced by deleting S as $G \setminus S$. An edge $(u, v) \in E$ can be *contracted* by adding a new node uv , adding edges from uv to all neighbors of u and v , then deleting u and v . A graph P is a *minor* of a graph H if P can be obtained from H with vertex deletion, edge deletion, and edge contraction. In the context of quantum annealing, we denote the graph P as a *problem graph* and H as a *hardware graph*.

ODD CYCLE TRANSVERSAL (OCT) is formally defined as an optimization problem with natural parameter k .

ODD CYCLE TRANSVERSAL (OCT)

Input: An input graph $G = (V, E)$.
Problem: Find $S \subseteq V$ such that $G \setminus S$ is bipartite.
Objective: Minimize $k := |S|$.

OCT is closely related to VERTEX COVER (VC).

VERTEX COVER (VC)

Input: An input graph $G = (V, E)$.
Problem: Find $S \subseteq V$ such that $G \setminus S$ is edgeless.
Objective: Minimize $|S|$.

Specifically, given a graph G , we create an auxiliary graph G' with two copies of G (which we call left and right) joined by a matching between corresponding vertices. Formally, $G' = (V_L \cup V_R, E_L \cup E_R \cup E')$, where for $i \in \{L, R\}$, $V_i = \{v_i \mid v \in V\}$ and $E_i = \{(u_i, v_i) \mid (u, v) \in E\}$, and $E' = \{(v_L, v_R) \mid v \in V\}$ is the matching edges. A solution S' for VC on G' can be mapped to a solution S for OCT on G with $S = \{v \mid v_L \in S \text{ and } v_R \in S\}$; this mapping preserves optimality [Akiba and Iwata 2016].

Both OCT and VC can also be rewritten as INTEGER LINEAR PROGRAMMING (ILP) instances; as explored further in Section 3.5, the choice of OCT \rightarrow ILP formulation has performance implications.

ODD CYCLE TRANSVERSAL (ILP) [HÜFFNER 2009]

Input: $G = (V, E)$.

$$\begin{aligned}
 & \text{Minimize} && \sum_{v \in V} c_v \\
 & \text{s.t.} && s_v + s_u + c_v + c_u \geq 1 && \forall (u, v) \in E \\
 & && s_v + s_u - c_v - c_u \leq 1 && \forall (u, v) \in E \\
 & && s_v \in \{0, 1\} && \forall v \in V \\
 & && c_v \in \{0, 1\} && \forall v \in V
 \end{aligned}$$

VERTEX COVER (ILP) [AKIBA AND IWATA 2016]

Input: $G = (V, E)$.

$$\begin{array}{ll} \text{Minimize} & \sum_{v \in V} x_v \\ \text{s.t.} & x_u + x_v \geq 1 \quad \forall (u, v) \in E \\ & x_v \in \{0, 1\} \quad \forall v \in V \end{array}$$

An *anytime algorithm* will return the best solution found so far when given a timeout signal. An *exact algorithm* will return a (provably) optimal solution, whereas a *heuristic* is unable to prove optimality. A middle ground between heuristic and exact is an *approximation algorithm*, whose error is bound with a constant. An α -approximation algorithm for a minimization problem has solution size k bounded by $k \leq \alpha \cdot OPT$, where OPT is the optimal solution size; α is the *approximation factor*. We define the approximation factor over a corpus of graph instances as the worst factor over all individual instances in the corpus.

2.1 Graph bipartization in quantum annealing

Recent advances in quantum computing has resulted in a class of optimization problem solvers denoted *quantum annealers* (QA). Implementations of QA hardware are based off of the adiabatic quantum annealing (AQC) model, but are typically less powerful (i.e. not universal quantum computers). These QA devices have *hardware topologies*, these graphs define the communication pathways (edges) between qubits (vertices). For example, D-Wave Systems currently produces QA hardware with Chimera hardware, and is preparing for a second generation Pegasus model.

Graph bipartization (OCT) occurs during the compilation step in quantum annealing, when a problem graph representing the optimization problem being solved by the quantum computer³ must be *embedded* as a minor into the graph representing the quantum hardware [Choi 2011]. Researchers have had success running naturally bipartite QUBOs (e.g. deep learning models) on D-Wave Systems annealers [Boyda et al. 2017; Kosko 1988; Potok et al. 2018; Schrock et al. 2017]. Generalizing these tools to non-bipartite QUBOs is currently of interest to enable additional applications (e.g. Karp’s 21 NP-hard problems [Lucas 2014]). The area of automatic embedding tools is under active development (refer to, e.g., [Goodrich et al. 2018b; Hamilton and Humble 2017; Venturelli et al. 2015]).

We examine two distinct use cases of graph bipartization in quantum program compilation.

First, a feasible bipartization of a graph is useful for certain embedding algorithms [Goodrich et al. 2018b; Hamilton and Humble 2017], providing a structure on which to limit the search space of heuristics. In this use case, an automated compiler might require this bipartization in as little as 0.01 seconds, whereas a computer-assisted researcher working in an interactive environment may wait closer to 10 seconds.

Second, OCT can be used to identify when a particular program cannot embed into hardware, as is shown for D-Wave Systems’ *Chimera* hardware in [Goodrich et al. 2018b]. This scenario requires that the solver return a certified optimal OCT solution, but longer run times are permissible since a hardware owner can compute forbidden configurations once per hardware model. We examine both of these use cases in more detail in Section 5.

³e.g. a QUADRATIC UNCONSTRAINED BINARY OPTIMIZATION (QUBO)

3 ALGORITHM OVERVIEW

In this section, we overview various algorithmic techniques previously applied to OCT. We begin with reduction routines from both the OCT and VC literature, then continue to linear-time heuristics historically used to provide upper bounds for branch-and-bound approaches. The first exact solver we detail is Hüffner’s iterative compression solver [Hüffner 2006], which we enhance with heuristics to create an anytime algorithm with increased performance particularly when given small timeouts. Finally, we detail how CPLEX can solve OCT using various reformulations into INTEGER LINEAR PROGRAMMING.

3.1 Reduction Routines

We begin with *reduction routines* – rules for simplifying the graph instance such that a solution on the reduced instance is valid for the original instance. Typically these reductions will remove vertices by recognizing configurations that can be simplified deterministically. Reduction routines for OCT come from two sources. Wernicke’s branch-and-bound algorithm [Wernicke 2003] uses nine reductions directly on the OCT instance. These reductions form roughly three categories: removal of standalone structures (e.g., bipartite components and degree-1 vertices), removal of vertex separators which induce certain bipartite components, and reconfigurations of local structures (e.g., removing a degree-2 vertex in an induced four-cycle). These reductions are most effective on close-to-bipartite graphs, low-connectivity graphs, and sparse graphs, respectively.

A second source of reductions is Akiba and Iwata’s VC solver [Akiba and Iwata 2016], which uses nine reduction routines specific to the VC instance’s graph. Based on the conversion between OCT and VC in Section 2, a vertex v in the OCT instance must be in the transversal if both v_1 and its mirror v_2 must be in the vertex cover in the VC instance. Similarly, v is labeled bipartite if v_1 or v_2 is excluded from an optimal vertex cover.

We refer the interested reader to the original papers [Akiba and Iwata 2016; Wernicke 2003] for detailed definitions, examples, and complexity analysis. We provide an open source implementation of Wernicke’s reductions using Python and NetworkX, and modify a copy of Akiba and Iwata’s VC solver [Akiba and Iwata 2017] to output the graph after a single round of reductions.

3.2 Heuristics and Approximations

Heuristics for OCT typically compute a maximal bipartite induced subgraph, then label all remaining vertices as an odd cycle transversal. One strategy for finding a large bipartite subgraph is greedily 2-coloring the vertices using a depth-first search, and adding incompatible vertices to an OCT set as needed [Wernicke 2003]; this heuristic has a natural breadth-first search variant. Both of these methods are nondeterministic with respect to the choice of the initial vertex and the order in which neighbors are added to the search queue. Another approach is to find an independent set for the first partite set, then repeat for a second partite set, as in Luby’s Algorithm [Luby 1986]. Recent work showed that by using the minimum-degree heuristic for independent set, this strategy gives a d -approximation in d -degenerate graphs [Goodrich et al. 2018b]. Both of these methods are nondeterministic; the former is stochastic by design, and the latter breaks ties between minimum degree vertices. We provide C++ implementations of these four heuristics (DFS, BFS, Luby, and MinDeg), and provide a *heuristic ensemble* solver that runs the heuristics round-robin until a specified timeout is reached.

3.3 Iterative Compression

The state-of-the-art implementation for solving OCT combinatorially comes from Hüffner’s simplification of the iterative compression algorithm [Hüffner 2009; Reed et al. 2004]. Broadly, the iterative compression technique starts with a trivial solution on a subgraph of the instance, expands both the solution and subgraph, then applies a compression routine to reduce the solution if possible. By iterating this process, the subgraph eventually encompasses the full graph, and the solution at every step is compressed to remain within some desired bound. The compression routine may have run time exponential in the size of the solution and is applied at most a linear number of times, naturally leading to an FPT algorithm parameterized by the solution size k .

In the specific application to OCT, the compression routine tries all $O(3^k)$ partitions of a $(k + 1)$ -sized solution into a new transversal and left/right partite sets. For each partition, an OCT set for the full subgraph is computed by solving a min-cut instance. If the number of vertices assigned to the transversal plus the vertices removed by the cut is less than $k + 1$, then the solution was compressed, and otherwise a certificate is found that no solution of size k exists on this subgraph. Using Edmonds-Karp for the min-cut algorithm, this compression routine runs in $O(3^k \cdot k \cdot |E|)$.

The iterating outer loop that expands the solution and subgraph is trivial for OCT: Given an ordering of the vertices, the initial subgraph and solution are the first k vertices, and the subgraph and solution are both expanded by adding the next unused vertex in the ordering to each. In the worst case there are n iterations, resulting in a total run time of $O(3^k \cdot k \cdot |V| \cdot |E|)$.

3.4 Modifications to Hüffner’s Algorithm

While Hüffner’s reformulation of Reed et al.’s algorithm was based on improving the compression routine, we note some straightforward improvements to the outer loop that can also lead to improvements in practice. These improvements are related to the choice of vertex ordering.

First, the number of compressions can be reduced by choosing an initial subgraph larger than the initial solution of size k . Specifically, given a heuristic solution S for OCT, we can construct an initial subgraph of size $\min(|V| - |S| + k, |V|)$ by placing the vertices in $V \setminus S$ first in the ordering, then initializing the subgraph with this bipartite subgraph and up to k of the remaining vertices. This ‘bipartite jump-start’ has no negative effect on the theoretical run time, but may improve run time by up to a factor of $|V|$ based on the quality of the heuristic solution.

Second, Hüffner’s improvements to the compression routine utilize the presence of edges to eliminate possible partitions from consideration. Namely, two vertices cannot be assigned to the same partition if they share an edge, and the number of partitions can be reduced from $O(3^k)$ in the worst case (an independent set) to $O(k^2)$ in the best case (a clique). To exploit this fact, after the ordering is jump-started with a bipartite subgraph, we order the remaining vertices in a reverse degeneracy ordering [Lick and White 1970]. This ordering guarantees that vertices added to the subgraph maximize the number of newly introduced edges.

Finally, we note that iterative compression is naturally an anytime algorithm. If, at any point, the iteration stops, the current solution size is a lower bound on the optimal OCT, and the current solution plus the vertices not yet reached in the ordering form an upper bound. By its FPT nature, the iterative compression approach becomes hard when k becomes large. However, iterative compression may fill an important niche between heuristics and exact solvers by offering a structured approach for compressing heuristic solutions as time allows.

We provide a modified copy of Hüffner’s implementation with both improvements implemented in C++ and enable anytime functionality when given a termination signal. Based on small-scale experimentation (Appendix C.2), we find

that the bipartite jump-start always helps in expectation, but the degeneracy ordering may not be worth the additional run time when using a small timeout. In our experiments we use only the first improvement on timeouts of 0.01 and 0.1 seconds, and otherwise we use both improvements.

3.5 Alternative Solvers

As mentioned in Section 2, OCT can be converted into an equivalent VERTEX COVER (VC) or INTEGER LINEAR PROGRAMMING (ILP) instance.

Currently, the fastest theoretical run time for OCT and other related problems comes from a VC-formulation [Loksh-tanov et al. 2014]. We evaluate this approach with Akiba and Iwata’s Java solver, which was previously demonstrated to be faster than Hüffner’s iterative compression algorithm [Akiba and Iwata 2016]. We implement a Python wrapper that converts between OCT and VC, providing a common API with the other solvers.

When solving OCT as an ILP, the instance can be directly converted $OCT \rightarrow ILP$, or converted with $OCT \rightarrow VC \rightarrow ILP$. In addition to choosing a formulation, the user must also choose an ILP solver (e.g. CPLEX or GLPK) and consider the effect of additional threads and/or RAM limitations. Testing several configurations (Appendix C.1), we confirmed several best practices from previous work. The biggest factor was choice of solver, where IBM’s closed-source CPLEX solver bested the open-source GNU solver GLPK. The next factor with the biggest impact was choice of formulation, where $OCT \rightarrow VC \rightarrow ILP$ performed significantly better than $OCT \rightarrow ILP$; this performance difference may be explained by a similar result in theoretical analysis [Loksh-tanov et al. 2014].

When evaluating the scalability of CPLEX on server hardware, we found that using multiple threads may lead to super-linear speed-up, and that while RAM limitations may increase run time, they do not change the relationship between other factors. In our experiments, we use the $OCT \rightarrow VC \rightarrow ILP$ formulation with the CPLEX solver, a single thread, and unrestricted RAM. Additionally, CPLEX allows recovery of partial solutions, enabling us to use this approach as an anytime algorithm. We again provide a Python wrapper for a common API.

4 DATA BENCHMARK AND CODE

In this section we detail the data used in the experiments, along with the code made available at [Goodrich et al. 2018a].

4.1 Previous Data

As mentioned in Section 1.1, the primary dataset studied in OCT literature originates from Wernicke and is distributed with Hüffner’s code. We refer to this data as the Wernicke-Hüffner (WH) dataset. These datasets are originally from genetics through the related MINIMUM SITE REMOVAL problem [Wernicke 2003] and are expected to be close to bipartite. This dataset is composed of 45 Afro-American graphs (denoted aa-10, . . . , aa-54) and 29 Japanese graphs (denoted j-10, . . . , j-28). Files aa-12, j-12, and j-27 are provided in Hüffner’s code, but are empty and excluded here.

4.2 Quantum-Inspired Data

While the WH dataset may have been of historical interest, recent results show that any state-of-the-art solver can solve all these instances within three seconds [Akiba and Iwata 2016]. To introduce a new benchmark corpus for OCT solvers, we concentrate on domain data from quantum computing. Specifically, a recent survey [Dunning et al. 2015] collected six datasets from the QUBO literature (see Section 2); of these, only the Beasley [Beasley 1998] and GKA [Glover et al. 1998] data have instances small enough to embed in near-term quantum annealing hardware.

In this work we consider the 50-vertex instances (denoted b-50-1, . . . , b-50-10) and the 100-vertex instances (denoted b-100-1, . . . , b-100-10) from the Beasley dataset and the first 35 instances of the GKA dataset (denoted gka-1, . . . , gka-35), which have varying numbers of vertices and densities (c.f., Table 1). All QUBO datasets are parsed as undirected, simple graphs with no vertex or edge weights. Vertices, edges with weight zero, and self-loops are excluded.

Additionally, we examine frustrated cluster loop (FCL) graphs. FCLs are generated by overlaying cycles from random walks on a base graph and were originally introduced as a benchmark for quantum annealing hardware that produced QUBO instances with *rugged* energy landscapes [King et al. 2019]. Rugged landscapes are characterized by having frequent, tall energy barriers, which reduces the effectiveness of classical solvers and makes use of quantum tunneling.

We use the D-Wave NetworkX API to generate a corpus of FCL instances applicable to four hardware models: a D-Wave 2000Q (16 × 16 Chimera grid), a theoretical D-Wave “8000Q” (32 × 32 Chimera grid), the upcoming Pegasus-6 (which embeds a $K_{52,52}$), and a Pegasus-12 (which embeds a $K_{124,124}$). For each hardware, we generated a corpus of FCLs from a clique of size n for a subset of the values between the size of the maximum clique embedding of the hardware and the size of the maximum biclique embedding of the hardware. See Appendix B for step sizes. We also varied the number of cycles used in each FCL from 5-30% of the base clique size to ensure a diverse set of FCL instances in the regime where OCT-embedding methods would be deployed. For example, the D-Wave 2000Q can embed a 64-clique and a 128-biclique, so we generate FCLs using cliques of size 64, 80, 96, 112, and 128; as seen in Figure 3 in Appendix B, the varied number of cycles results in a corpus of instances with good coverage of the desired size interval [64, 128].

Due to similarity between the graph instances sizes, we further cluster the 2000Q and Pegasus-6 FCL graphs into a fcl-small corpus and the 8000Q and Pegasus-12 into fcl-large.

4.3 Synthetic Graph Generators

To generalize our results and prevent bias that may be present in a difficult QUBO benchmark, we use synthetic graph generators to mimic distinct properties of the quantum graphs.

To match edge density, we use the Erdős-Rényi model [Erdos and Rényi 1960], which takes as input a number of vertices n and a probability p . Erdős-Rényi generates a graph by initializing n vertices and adding each edge with probability p . By setting $p := |E|/\binom{n}{2}$ we have the same edge density in expectation.

To mimic a dataset’s distance-to-bipartite, we provide a Tunable-OCT generator as a modification of Erdős-Rényi. The Tunable-OCT generator requires an upper bound on the optimal OCT solution (denoted n_o) and a bipartite balance parameter $0 \leq b \leq 1$. Tunable-OCT generates a graph by partitioning the vertices into an odd cycle transversal, a left partite set, and a right partite set. The odd cycle transversal has n_o vertices, and the remaining vertices are assigned to the left partite set with probability b . Edges are then generated according to Erdős-Rényi, with the exception that vertices in the same partite set may not share an edge. This construction enforces that $OPT \leq n_o$, highlighting the distinction between arbitrary edge placements and a potentially small optimal OCT solution. In our experimental results we set n_o equal to the optimal solution for the original (non-preprocessed) graphs, and set $b = 0.5$.

For matching degree distribution in addition to density we use the Chung-Lu expected degree model [Chung and Lu 2002]. Given a degree distribution (d_1, \dots, d_n) , the Chung-Lu model adds an edge uv with probability

$$P_{uv} = \frac{d_u d_v}{\sum_{i=1}^n d_i}.$$

We generate these graphs using the original instances’ degree distribution.

Dataset	Original Graph		Reductions					Reduced Graph	
	$ V $	$ E / V $	$ \widehat{V}_r $	$ \widehat{E}_r $	$ \widehat{V}_o $	$ \widehat{V}_b $	Solved	$ V' \cup V_b $	$ E' / V' \cup V_b $
WH-aa	39–300	1.8–5.4	13%	-	-	70%	11%	27–265	1.9–6.1
WH-j	33–150	1.5–5.9	29%	-	-	13%	23%	8–74	2.0–7.5
b-50	50	2.0–2.7	2%	-	-	4%	-	43–50	2.1–2.7
b-100	100	4.6–5.1	-	-	-	-	-	100	4.6–5.1
gka	20–125	2.1–61.3	-	-	9%	-	11%	6–100	2.0–43.5

Table 1. A summary of preprocessing statistics on WH and quantum datasets. Ranges are given for the number of vertices and edge density in both the original and reduced graphs. The statistic $|\widehat{V}_r|$ reports the percentage of vertices removed on average. Likewise, normalized means are reported for edge removals E_r , fixed-OCT vertices V_o , and fixed-bipartite vertices V_b ; dashes denote zero changes. The percentage of graphs solved completely by preprocessing routines is also reported.

Finally, we also include the Barabási-Albert preferential attachment model [Albert and Barabási 2002] to highlight the effect of a severely biased degree distribution at fixed edge density. Given a set of initial vertices, a constant c , and a number n of additional vertices, each new vertex is added to the graph with c edges attached to the existing nodes with probability proportional to their current degree. We match the original graphs’ number of vertices and select c such that the same number of edges are added (up to integer rounding).

4.4 Replicability

All experiments are fully replicable with our open source code repository [Goodrich et al. 2018a]. After installing the software with the README instructions, we direct the interested reader to REPLICABILITY.md for detailed instructions.

To sanitize the data, graphs are relabeled with vertices $\{0, \dots, n - 1\}$ and are written to files for each solver’s required format. The reduction routines are natively nondeterministic, but data is explicitly sorted in both OCT- and VC-based routines such that a single run will generate identical results on distinct hardware and software environments.

All algorithms are available as standalone solvers using a command-line interface, and Python scripts are provided for reproducing the experiments, including tables and plots.

5 QUANTUM-SPECIFIC RESULTS

5.1 Experimental Setup

All experiments were run on three identical Dell PowerEdge R430 servers, each with an Intel E5-2623 v2 CPU (3.5GHz single-core turbo, 10MB cache) and 64GB ECC DDR4 RAM. Each server ran Fedora 27 with Linux kernel 4.16.7, CPLEX 12.8, and GLPK 4.61. C and C++ code were compiled with Clang version 5.0.1, Java code was compiled with OpenJDK 1.8.0_181, and Python code was run with Python 3.5.6 (restricted by CPLEX 12.8).

5.2 Preprocessing Effectiveness

In this subsection we harden the benchmark by applying the reduction routines detailed in Section 3.1. We denote reductions as a partition of the original vertex set $V = V_r \uplus V_o \uplus V_b \uplus V'$. The vertices that may be removed without changing OCT are denoted V_r . For some fixed optimal solution S , vertices V_o must be in S and vertices V_b cannot be in S . Finally, the remaining vertices are labeled V' . Analogously, the edges are partitioned into $E = E_r \uplus E'$. The sets V_r , E_r , and V_o may be safely removed from the graph, leaving the reduced graph with vertices $V_b \cup V'$ and edges E' .

Dataset	0.01(s)			0.1(s)			1(s)			10(s)		
	HE	IC	ILP	HE	IC	ILP	HE	IC	ILP	HE	IC	ILP
WH-aa	1.54	1.57	24.25	1.33	1.24	2.10	1.29	1.29	1.25	1.24	1.08	✓
WH-j	1.11	✓	3.92	1.11	✓	✓	✓	✓	✓	✓	✓	✓
b-50	1.11	1.09	1.67	1.11	✓	1.21	1.08	✓	✓	✓	✓	✓
b-100	1.07	1.10	2.10	1.07	1.10	1.34	1.05	1.07	1.15	1.05	1.05	1.05
gka	1.18	1.21	2.36	1.18	1.21	1.36	1.11	1.11	1.17	1.11	1.11	1.07
fcl-small	1.50	1.41	5.00	1.50	1.29	1.57	1.33	1.20	1.18	1.23	1.18	1.09
fcl-large	1.71	1.50	5.00	1.53	1.42	2.33	1.43	1.35	1.48	1.38	1.29	1.21

Table 2. Observed approximation factors for anytime algorithms: the heuristic ensemble (HE), iterative compression (IC), and integer linear programming (ILP). For each dataset, the worst-case approximation ratio over its instances is reported. Approximation ratios are with respect to OCT on the reduced graph, computed with ILP. A checkmark denotes that exact solutions are found on all instances, if a dataset has no checkmark then the best approximation algorithm is bolded.

Table 1 summarizes preprocessing results over the non-synthetic datasets. We observe that the reduction routines’ effectiveness is dataset-dependent. The WH data is amenable to vertex removals, particularly WH-j, which had its largest graph reduced from 241 to 74 vertices. Perhaps due to a very low edge density, the WH-aa also had a significant number of vertices labeled bipartite. The GKA dataset was only affected by reductions that fixed OCT vertices, which can be important for exact algorithms fixed-parameter tractable in the solution size. Few reductions applied to the Beasley data, with b-100 remaining untouched. Both WH and GKA data contained instances that were completely solved by preprocessing.

5.3 Use Case: Heuristic Solutions

For the first quantum use case, an embedding compiler may need a bipartization of an input program (e.g., a QUBO or circuit) in order to prune a search space of embeddings, but has very little time budgeted for this step. Therefore we compare the best (potentially non-optimal) solutions found per solver with fixed timeouts. The algorithms capable of producing heuristic solutions are the heuristic ensemble (HE), the improved iterative compression solver (IC), and the ILP formulation with CPLEX (ILP). To evaluate the heuristics and anytime algorithms in this scenario we choose timeouts of four different orders of magnitude (0.01, 0.1, 1.0, and 10 seconds). At the timeout, each algorithm is given a termination signal and is given time to output the last solution cached.

Table 2 reports the worst-case approximation factors achieved by an algorithm-data-timeout triple; full results on the WH, Beasley, and GKA data are reported in Appendix C (Tables 8 and 9). We observe that for very short timeouts, the HE and IC solvers noticeably outperform the ILP solver in terms of solution quality, achieving worst-case approximation factors of at most 1.57 for all data with timeouts of 0.01(s) and 0.1(s). At the other end of the spectrum, for a timeout of 10s, ILP is the dominant solver with a worst-case approximation factor of 1.21. Between these two at a timeout of 1s, the best approach is not clear. We also note that the approximation factors for the FCL datasets are consistently larger than those of the non-synthetic data.

5.4 Use Case: Exact Solutions

In the second use case, a researcher may want a ‘litmus test’ evaluating whether a program’s structure can be represented in a given quantum hardware. By recognizing that the OCT size of a problem graph is too large, we can show that

Graph		Solver			Graph		Solver		
Dataset	OPT	VC	IC	ILP	Dataset	OPT	VC	IC	ILP
b-100-1	41	101.5	-	79.5	gka-21	40	1.5	31.2	0.6
b-100-2	42	190.8	-	159.2	gka-22	43	5.0	-	6.5
b-100-3	42	252.8	-	58.0	gka-23	46	44.5	-	63.2
b-100-4	41	212.7	-	176.8	gka-24	37	76.6	-	95.8
b-100-5	42	217.6	-	246	gka-25	42	130.6	-	169.6
b-100-6	43	150.1	-	223.3	gka-26	43	168.2	-	113.6
b-100-7	42	189.0	-	270.1	gka-27	62	555.1	-	477.3
b-100-8	43	368.7	-	209.6	gka-28	70	300.8	-	516.1
b-100-9	44	333.5	-	470.5	gka-29	77	67.1	-	423.0
b-100-10	44	195.4	-	478.4	gka-30	82	33.6	-	305.2
gka-3	23	1.5	273.4	4.4	gka-31	85	12.4	109.6	91.9
gka-8	28	7.2	-	8.5	gka-32	88	5.4	18.8	40.3

Table 3. Run times (in seconds) of exact solvers on a representative sample of Beasley and GKA data with a 10 minute timeout. Algorithm-data pairings that did not finish within the timeout are denoted with a dash, and the best run time on a dataset is bolded.

such a configuration is impossible to embed in this hardware topology. We simulate this use case by computing exact solutions with a 10 minute timeout on preprocessed instances using the three solvers that could guarantee optimality: the VC-solver (VC), iterative compression (IC), and ILP (ILP).

We find that the solvers are fairly evenly split on total run time victories (Table 3), with ILP performing better on the Beasley data and VC performing better on GKA. Iterative compression only finished a handful of times within 10 minutes, and only once was competitive (gka-32).

Based on these results, we chose to only run the VC-solver and ILP on the FCL data. As seen in Figure 1, the ILP solver was dominant. While the VC-solver was faster on a few fcl-large instances, this does not appear to be correlated with the minimum OCT size.

6 GENERALIZED RESULTS

In this section, we expand the experimental envelope further by taking each WH and quantum dataset and creating several “look-a-likes” – synthetic graphs that match the original in different facets. We use the Erdős-Rényi generator to match density, the Tunable-OCT model to match proximity to bipartite, the Chung-Lu model to match degree distribution, and Barabási-Albert to increase degree distribution heterogeneity at a fixed edge density; all models and parameter settings are detailed in Section 4.3. A single synthetic instance is generated from a quantum instance, a synthetic graph generator, and a pseudorandom number generator seed. 15 seeds are used for the preprocessing and heuristic experiments, and 5 seeds are used for the (computationally expensive) exact results.

6.1 Reduction Effectiveness

Table 4 depicts the effectiveness of reduction routines on the synthetic data. Across most datasets, the Tunable-OCT and Chung-Lu synthetic graphs resulted in more vertex removals than the original graphs. In the case of WH-aa, this increase in V_r also involved a drastic decrease of vertices labeled bipartite (V_b). Again, the Beasley datasets remained relatively unaffected by reduction, excepting the Tunable-OCT analogues for b-50.

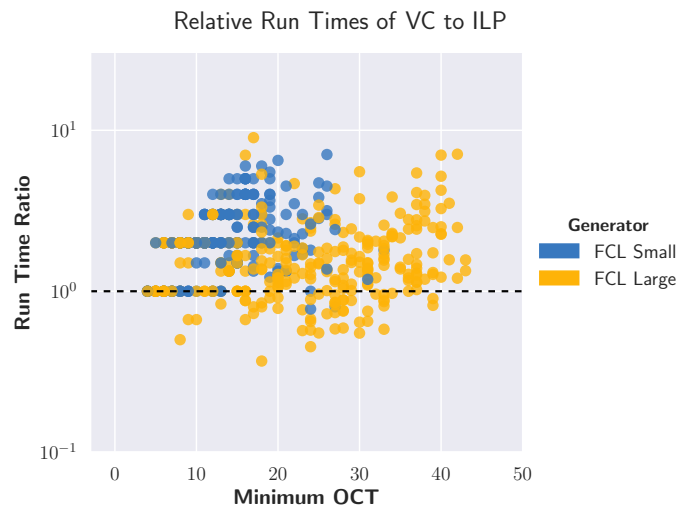


Fig. 1. Plot of VC-solver time divided by ILP solver time for exact solutions on FCL graphs. Points above the dashed line indicate the ILP formulation outperforms the equivalent VC formulation, and include almost all of the `fc1-small` instances.

6.2 Heuristic Solutions

When extending the heuristic solution comparison to synthetic data, we find the same best practices generally still apply (Table 5). At 0.01s, IC has little time to improve on the initial heuristic solution and so the quick solutions found by HE remain competitive. At 0.1s and 1s, HE begins to have diminishing returns and the compression steps towards an exact solution begin to pay off for IC. At 1s, ILP also begins to produce winning solutions, solving all of `b-50` and splitting the wins otherwise. Finally, with 10s to execute the full CPLEX reduction routines, ILP begins to dominate.

We observe that over all data and algorithms, 0.01 seconds is enough to get a 2.70-approximation (and 1.42 outside of `WH-aa-to`) with IC; 0.1 seconds yields a 1.79-approximation with IC; 1 second yields a 1.65-approximation with IC, and 10 seconds yields a 1.14-approximation with ILP. From a domain-science standpoint, these relatively small errors show that OCT can be considered a practical subroutine when searching for a ‘good enough’ solution in a time-sensitive environment.

6.3 Exact Solutions

Expanding on Table 3, we find that the choice between ILP and VC is heavily dataset- and generator-dependent. Notably, in the first facet of Figure 2 we find that `Tunable-OCT` data is difficult for the VC-solver and CPLEX can solve the instances up to $1000\times$ faster. However, the `Barabási-Albert` instances are similarly easier for a VC-solver. The effectiveness of branch-and-reduce algorithms on instances with heavy-tailed degree distributions is well-known in folklore – the few high-degree vertices in this network result in few branches, and the remaining (sparse) graph can sometimes be solved by reduction routines alone. The results for `WH-j` and `GKA` are also split fairly evenly, although the latter has no clear split by generator. Notably, `GKA` has instances with very large OCT that are best solved with ILP; in the rest of the data VC tends to perform best as minimum OCT increases. The `b-50` and `b-100` corpuses are best solved by ILP and VC, respectively.

Dataset	Original Graph		Reductions					Reduced Graph	
	$ V $	$ E / V $	$ \widehat{V}_r $	$ \widehat{E}_r $	$ \widehat{V}_o $	$ \widehat{V}_b $	Solved	$ V' \cup V_b $	$ E' / V' \cup V_b $
WH-aa	39–300	1.8–5.4	13%	-	-	70%	11%	27–265	1.9–6.1
WH-aa-ER	15–300	1.2–5.6	1%	-	-	2%	4%	10–300	1.4–5.6
WH-aa-TO	27–300	0.9–4.1	15%	-	-	12%	8%	10–299	1.4–4.1
WH-aa-CL	27–300	1.3–5.5	55%	-	6%	12%	9%	9–155	1.5–6.7
WH-aa-BA	14–300	1.7–5.9	1%	-	-	1%	8%	7–300	1.4–5.9
WH-j	33–150	1.5–5.9	29%	-	-	13%	23%	8–74	2.0–7.5
WH-j-ER	33–241	1.1–6.3	6%	-	-	4%	13%	18–239	1.5–6.3
WH-j-TO	33–150	0.8–4.1	17%	-	-	7%	32%	10–104	1.4–4.1
WH-j-CL	33–241	1.2–6.2	39%	-	4%	7%	22%	10–138	1.5–7.5
WH-j-BA	33–241	1.9–5.6	7%	-	1%	4%	14%	10–241	1.3–5.7
b-50	50	2.0–2.7	2%	-	-	4%	-	43–50	2.1–2.7
b-50-ER	50	1.7–3.3	3%	-	-	3%	-	31–50	1.9–3.4
b-50-TO	50	1.2–2.5	14%	-	-	6%	3%	13–48	1.4–2.7
b-50-CL	50	1.7–3.0	8%	-	1%	4%	-	24–49	1.8–3.2
b-50-BA	50	2.8	4%	-	2%	5%	6%	30–50	1.9–2.8
b-100	100	4.6–5.1	-	-	-	-	-	100	4.6–5.1
b-100-ER	100	4.3–5.5	-	-	-	-	-	98–100	4.3–5.5
b-100-TO	100	3.6–4.8	-	-	-	1%	-	95–100	3.6–4.8
b-100-CL	100	4.1–5.5	1%	-	-	1%	-	95–100	4.2–5.5
b-100-BA	100	4.8–5.6	-	-	-	-	-	98–100	4.3–5.7
gka	20–125	2.1–61.3	-	-	9%	-	11%	6–100	2.0–43.5
gka-ER	20–125	1.8–61.4	-	-	9%	-	13%	6–100	1.9–43.7
gka-TO	20–125	1.2–61.4	1%	-	12%	1%	8%	6–100	1.6–43.6
gka-CL	20–125	1.7–60.9	1%	-	10%	-	11%	6–100	1.7–43.2
gka-BA	20–125	2.8–31.2	-	-	1%	-	1%	9–123	1.6–29.9

Table 4. A summary of preprocessing statistics over all datasets. Ranges are given for the number of vertices and edge density in both the original and reduced graphs. The normalized statistic $|\widehat{V}_r|$ reports the average percentage of vertices removed. Likewise, normalized means are reported for edge removals E_r , fixed-OCT vertices V_o , and fixed-bipartite vertices V_b ; dashes denote zero changes. The percent of graphs per dataset completely solved by preprocessing routines is also noted. Results are reported over 15 seeds per random graph generator, per original dataset.

Overall, ILP generally does best on graphs with small minimum OCT (≤ 25), otherwise VC returns faster solutions. The results in WH-aa and WH-j also suggest that Tunable-OCT is best solved with ILP; extended work could evaluate whether these datasets are particularly easy for ILP or particularly hard for VC.

7 CONCLUSION

We experimentally evaluate state-of-the-art approaches to computing ODD CYCLE TRANSVERSAL on the canonical WH dataset, a new benchmark dataset from quantum annealing, and synthetic data generated using four random graph models which emphasize different structural properties. Whereas previous experimental evaluations were limited to 61

Dataset	Timeout: Represented	0.01(s)			0.1(s)			1(s)			10(s)		
		HE	IC	ILP	HE	IC	ILP	HE	IC	ILP	HE	IC	ILP
WH-aa-er	61%	1.26	1.30	3.16	1.21	1.21	1.52	1.21	1.16	1.35	1.14	1.14	1.15
WH-aa-to	100%	2.41	2.70	15.00	1.95	1.79	5.75	1.65	1.65	3.11	1.54	1.56	✓
WH-aa-cl	100%	1.33	1.24	3.43	1.25	1.21	1.47	1.18	1.19	1.11	1.17	1.17	1.05
WH-aa-ba	86%	1.50	1.39	4.43	1.40	1.33	1.73	1.33	1.30	1.39	1.30	1.30	1.14
WH-j-er	93%	1.30	1.31	3.12	1.21	1.21	1.64	1.19	1.18	1.39	1.19	1.18	1.11
WH-j-to	100%	1.78	1.31	8.33	1.44	1.18	1.88	1.31	1.11	✓	1.15	✓	✓
WH-j-cl	100%	1.29	1.29	3.67	1.25	1.17	1.52	1.21	1.17	1.08	1.17	1.15	✓
WH-j-ba	100%	1.60	1.42	4.58	1.40	1.33	1.93	1.33	1.36	1.48	1.31	1.36	1.10
b-50-er	100%	1.33	1.17	2.00	1.18	1.08	1.31	1.12	1.07	✓	✓	1.07	✓
b-50-to	100%	1.25	1.10	2.25	1.20	1.14	1.22	✓	✓	✓	✓	✓	✓
b-50-cl	100%	1.20	1.17	1.75	1.17	1.12	1.27	1.14	1.08	✓	✓	1.08	✓
b-50-ba	100%	1.25	1.18	1.90	1.17	1.09	1.18	1.10	1.09	✓	✓	✓	✓
b-100-er	100%	1.10	1.19	2.12	1.10	1.10	1.40	1.07	1.07	1.21	1.07	1.07	1.09
b-100-to	100%	1.16	1.24	2.70	1.15	1.16	1.45	1.12	1.12	1.31	1.10	1.10	1.11
b-100-cl	100%	1.17	1.18	2.39	1.14	1.14	1.49	1.12	1.12	1.20	1.12	1.10	1.07
b-100-ba	100%	1.21	1.18	3.04	1.14	1.11	1.38	1.11	1.11	1.11	1.11	1.11	1.03
gka-er	99%	1.25	1.24	2.59	1.20	1.24	1.44	1.20	1.20	1.19	1.16	1.16	1.10
gka-to	100%	1.29	1.32	2.61	1.25	1.18	1.62	1.18	1.18	1.26	1.12	1.15	1.08
gka-cl	100%	1.22	1.24	3.14	1.18	1.15	1.39	1.12	1.17	1.24	1.09	1.12	1.07
gka-ba	100%	1.27	1.28	3.19	1.20	1.24	2.25	1.20	1.16	1.12	1.11	1.14	1.06

Table 5. Observed approximation factors for anytime algorithms and heuristics at various timeouts. For each dataset, the worst-case approximation ratio over its instances is reported. Approximation ratios are with respect to OCT on the reduced graph. A checkmark denotes that exact solutions are found on all instances, if a dataset has no checkmark then the best approximation algorithm is bolded. If OCT could not be found within 10 minutes then the instance is not included; the percent of included data points is denoted in the *represented* column.

graphs, each solved by modern methods within 1s, we utilize 116 existing benchmark instances, 840 frustrated cluster loop instances, and nearly 7000 synthetic instances from four different random graph generators.

On this significantly expanded corpus, we found that no single implementation dominates all scenarios. Under the most extreme time constraint of 0.01s, sampling from simple heuristics provides the best solutions. When using 0.1s, 1s, and 10s timeouts we find that a heuristic solution improved with structured work towards an exact solution performs best, including techniques such as iterative compression. After 10s, though, the preprocessing overhead of using CPLEX pays off and an ILP-solver dominates.

For significantly longer runs (a 10m timeout), we find IC uncompetitive and the choice between VC- and ILP-based solvers depends on the instance structure. We note that solvers may have inherent performance differences due to implementation language. However, we expect that the effectiveness of solvers heavily depends on potency of their preprocessing routines – CPLEX applies algebra-based reductions on the ILP before performing branch-and-cut, and Akiba and Iwata’s VC-solver applies reductions after each branch in their branch-and-reduce model. More work is needed in identifying (in)effective reduction routines based on instance structure. Results from the 2019 Parameterized

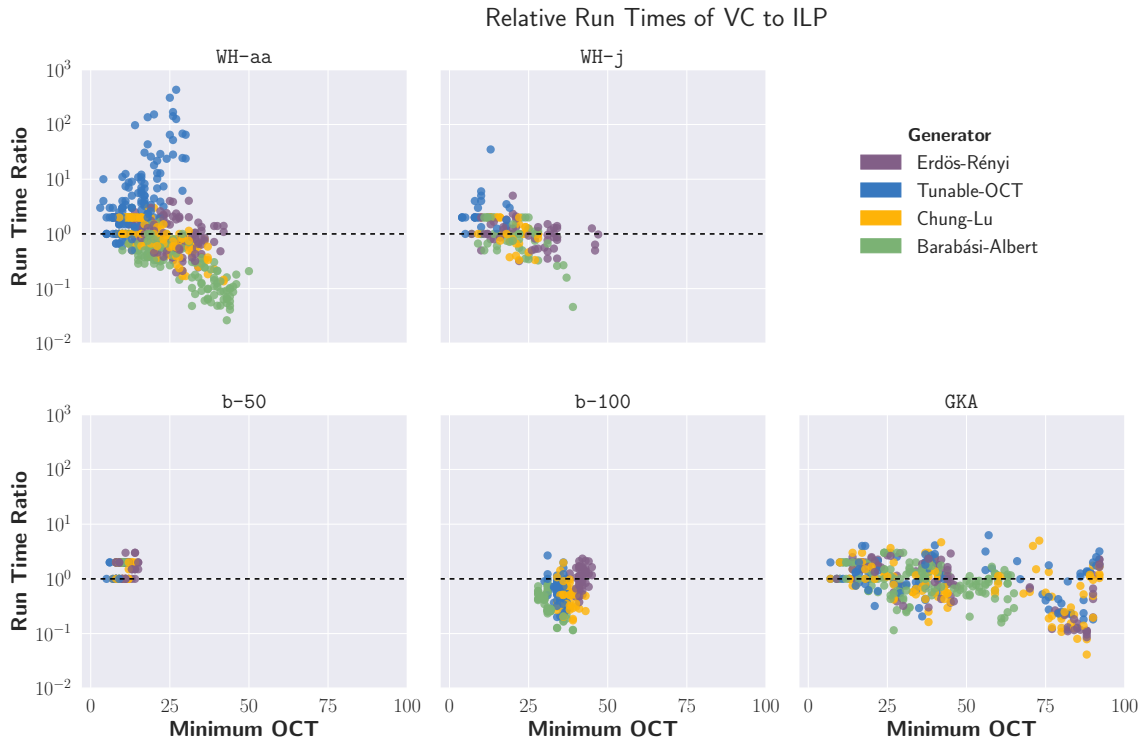


Fig. 2. Relative run times computed by dividing VC run times by those from ILP with one thread; the dashed line indicates equality. Data points reported over a synthetic corpus with five random generator seeds.

Algorithms and Computational Experiments (PACE) challenge⁴ for VERTEX COVER may be of particular interest towards this goal.

In addition to further study in preprocessing and structure of difficult instances, more flexible implementations are needed on the combinatorial algorithm front. Algorithms such as VC branch-and-reduce can be CPU-parallelized on a shared-memory system to potentially obtain super-linear speed-ups (witnessed by CPLEX in Appendix C). Techniques such as iterative compression may also lend themselves to GPU-parallelization by executing an exponential number of disjoint MINIMUM CUT subroutines in parallel.

In addition to parallelism, implementations should also be provided as anytime algorithms whenever possible. Many techniques create iteratively better lower bounds which can be completed into upper bounds with a simple rounding strategy. These “good enough” solutions are directly useful for applications such as quantum computing, and the lower bounds may be useful in their own right.

Acknowledgments. This work supported in part by the Gordon & Betty Moore Foundations Data-Driven Discovery Initiative through Grant GBMF4560 to Blair D. Sullivan, and with Government support under and awarded by DoD, Air Force Office of Scientific Research, National Defense Science and Engineering Graduate (NDSEG) Fellowship, 32 CFR 168a to Timothy D. Goodrich.

⁴<https://pacechallenge.org/2019/>

REFERENCES

- Amrit Agarwal, Moses Charikar, Konstantin Makarychev, and Yury Makarychev. 2005. $O(\sqrt{\log n})$ approximation algorithms for min UnCut, min 2CNF deletion, and directed cut problems. In *Proceedings of the thirty-seventh annual ACM symposium on Theory of computing*. ACM, ACM, New York, NY, USA, 573–581.
- Takuya Akiba and Yoichi Iwata. 2016. Branch-and-reduce exponential/fpt algorithms in practice: A case study of vertex cover. *Theoretical Computer Science* 609 (2016), 211–225.
- Takuya Akiba and Yoichi Iwata. 2017. Vertex Cover Solver. https://github.com/wata-orz/vertex_cover
- Réka Albert and Albert-László Barabási. 2002. Statistical mechanics of complex networks. *Reviews of modern physics* 74, 1 (2002), 47.
- John E. Beasley. 1998. Heuristic algorithms for the unconstrained binary quadratic programming problem.
- John E. Beasley. 2018. OR-Library. <http://people.brunel.ac.uk/~mastjjb/jeb/info.html>
- Edward Boyda, Saikat Basu, Sangram Ganguly, Andrew Michaelis, Supratik Mukhopadhyay, and Ramakrishna R Nemani. 2017. Deploying a quantum annealing processor to detect tree cover in aerial imagery of California. *PloS one* 12, 2 (2017), e0172505.
- Vicky Choi. 2011. Minor-embedding in adiabatic quantum computation: II. Minor-universal graph design. *Quantum Information Processing* 10, 3 (2011), 343–353.
- Fan Chung and Linyuan Lu. 2002. Connected components in random graphs with given expected degree sequences. *Annals of combinatorics* 6, 2 (2002), 125–145.
- Iain Dunning, Swati Gupta, and John Silberholz. 2015. What Works Best When? A Framework for Systematic Heuristic Evaluation. http://www.optimization-online.org/DB_FILE/2015/05/4895.pdf
- Paul Erdos and Alfréd Rényi. 1960. On the evolution of random graphs. *Publ. Math. Inst. Hung. Acad. Sci* 5, 1 (1960), 17–60.
- Fred Glover, Gary A. Kochenberger, and Bahram Alidaee. 1998. Adaptive memory tabu search for binary quadratic programs. *Management Science* 44, 3 (1998), 336–345.
- GNU. 2017. Linear Programming Kit (GLPK), Version 4.61. <http://www.gnu.org/software/glpk/glpk.html>
- Timothy D. Goodrich, Eric Horton, and Blair D. Sullivan. 2018a. Practical OCT. <https://doi.org/10.5281/zenodo.1493276>
- Timothy D. Goodrich, Blair D. Sullivan, and Travis S. Humble. 2018b. Optimizing adiabatic quantum program compilation using a graph-theoretic framework. *Quantum Information Processing* 17, 5 (07 Apr 2018), 118.
- Kathleen E. Hamilton and Travis S. Humble. 2017. Identifying the minor set cover of dense connected bipartite graphs via random matching edge sets. *Quantum Information Processing* 16, 4 (2017), 94.
- Falk Hüffner. 2006. occ. <http://theinfl.informatik.uni-jena.de/occ/>
- Falk Hüffner. 2009. Algorithm engineering for optimal graph bipartization. *Journal of Graph Algorithms and Applications* 13, 2 (2009), 77–98.
- IBM. 2017. CPLEX Optimization Studio 12.8. <https://www.ibm.com/analytics/data-science/prescriptive-analytics/cplex-optimizer>
- Yoichi Iwata, Keigo Oka, and Yuichi Yoshida. 2014. Linear-time FPT algorithms via network flow. In *Proceedings of the twenty-fifth annual ACM-SIAM symposium on Discrete algorithms*. Society for Industrial and Applied Mathematics, Society for Industrial and Applied Mathematics, Philadelphia, PA, USA, 1749–1761.
- Yoichi Iwata, Yutaro Yamaguchi, and Yuichi Yoshida. 2017. 0/1/all CSPs, Half-Integral A-path Packing, and Linear-Time FPT Algorithms.
- James King, Sheir Yarkoni, Jack Raymond, Isil Ozfidan, Andrew D King, Mayssam Mohammadi Nevisi, Jeremy P Hilton, and Catherine C McGeoch. 2019. Quantum annealing amid local ruggedness and global frustration. *Journal of the Physical Society of Japan* 88, 6 (2019), 061007.
- Bart Kosko. 1988. Bidirectional associative memories. *IEEE Transactions on Systems, man, and Cybernetics* 18, 1 (1988), 49–60.
- Stefan Kratsch and Magnus Wahlström. 2014. Compression via matroids: a randomized polynomial kernel for odd cycle transversal. *ACM Transactions on Algorithms (TALG)* 10, 4 (2014), 20.
- Don R Lick and Arthur T White. 1970. k-Degenerate graphs. *Canadian Journal of Mathematics* 22, 5 (1970), 1082–1096.
- Daniel Lokshantov, NS Narayanaswamy, Venkatesh Raman, MS Ramanujan, and Saket Saurabh. 2014. Faster parameterized algorithms using linear programming. *ACM Transactions on Algorithms (TALG)* 11, 2 (2014), 15.
- Daniel Lokshantov, Saket Saurabh, and Somnath Sikdar. 2009. Simpler parameterized algorithm for OCT. In *International Workshop on Combinatorial Algorithms*. Springer, Springer, Hradec nad Moravicí, Czech Republic, 380–384.
- Daniel Lokshantov, Saket Saurabh, and Magnus Wahlström. 2012. Subexponential Parameterized Odd Cycle Transversal on Planar Graphs. In *IARCS Annual Conference on Foundations of Software Technology and Theoretical Computer Science (FSTTCS 2012) (Leibniz International Proceedings in Informatics (LIPIcs))*, Deepak D’Souza, Telikepalli Kavitha, and Jaikumar Radhakrishnan (Eds.), Vol. 18. Schloss Dagstuhl–Leibniz-Zentrum fuer Informatik, Dagstuhl, Germany, 424–434. <https://doi.org/10.4230/LIPIcs.FSTTCS.2012.424>
- Michael Luby. 1986. A simple parallel algorithm for the maximal independent set problem. *SIAM journal on computing* 15, 4 (1986), 1036–1053.
- Andrew Lucas. 2014. Ising formulations of many NP problems. *Frontiers in Physics* 2 (2014), 5.
- Hartmut Neven, Geordie Rose, and William G. Macready. 2008. Image recognition with an adiabatic quantum computer I. Mapping to quadratic unconstrained binary optimization.
- Thomas E Potok, Catherine Schuman, Steven Young, Robert Patton, Federico Spedalieri, Jeremy Liu, Ke-Thia Yao, Garrett Rose, and Gangotree Chakma. 2018. A Study of Complex Deep Learning Networks on High-Performance, Neuromorphic, and Quantum Computers. *ACM Journal on Emerging Technologies in Computing Systems (JETC)* 14, 2 (2018), 19.

- Bruce Reed, Kaleigh Smith, and Adrian Vetta. 2004. Finding odd cycle transversals. *Operations Research Letters* 32, 4 (2004), 299–301.
- Jonathan Schrock, Alex J. McCaskey, Kathleen E. Hamilton, Travis S. Humble, and Neena Imam. 2017. Recall Performance for Content-Addressable Memory Using Adiabatic Quantum Optimization. *Entropy* 19, 9 (2017), 500.
- Davide Venturelli, Salvatore Mandra, Sergey Knysh, Bryan O’Gorman, Rupak Biswas, and Vadim Smelyanskiy. 2015. Quantum optimization of fully connected spin glasses. *Physical Review X* 5, 3 (2015), 031040.
- Magnus Wahlström. 2017. LP-branching algorithms based on biased graphs. In *Proceedings of the Twenty-Eighth Annual ACM-SIAM Symposium on Discrete Algorithms*. Society for Industrial and Applied Mathematics, Society for Industrial and Applied Mathematics, Philadelphia, PA, USA, 1559–1570.
- Sebastian Wernicke. 2003. On the algorithmic tractability of single nucleotide polymorphism (SNP) analysis and related problems.

A IMPLEMENTATION DETAILS

A.1 Data Ingestion and Sanitization

Original data comes from two sources. Wernicke-Hüffner data is provided in the Hüffner code download [Hüffner 2006], and Beasley and GKA data comes from Beasley’s repository [Beasley 2018].

When parsing the graphs with Python we read them into a NetworkX graph and remove edges with weight zero (used to denote non-edges in some problems) and self-loops. We then relabel the vertices to $\{0, \dots, n - 1\}$. To remove possible non-determinism in how vertices are relabeled, we specify that node labels are relabeled by lexicographical order of the original vertex labels, guaranteeing that each graph is always converted in the same way.

See the **Data** section of REPLICABILITY.md in our repository for information on how to use our scripts for automating this download and parsing process.

A.2 Reduction Routines

Reduction routines for preprocessing come from two papers: Wernicke [Wernicke 2003] and Akiba and Iwata [Akiba and Iwata 2016].

While Wernicke originally implemented his reductions in Java, the code does not appear to have been open sourced. We implement his reduction routines in Python3 with NetworkX. Some care must be taken that these reductions operate deterministically so the results can be reproduced. Specifically, reduction rules 4 and 6 require vertex cuts, which are returned in arbitrary order when computed by NetworkX; we convert the cuts to tuples and sort them by vertex label. Additionally, reduction rules 7, 8, and 9 find and remove particular configurations in the graph based on degree 2 and 3 vertices; we sort these sets of vertices and the related neighborhoods.

For Akiba and Iwata’s reduction routines, we modify their GitHub code [Akiba and Iwata 2017] so that no branching is done after the first iteration of reduction routines, and the preprocessed graph is output instead. To preprocess a graph, we apply Wernicke reductions first, then Akiba-Iwata reductions, and repeat until the graph does not change. This was done primarily because some of Akiba-Iwata’s reductions will not apply after the Wernicke reductions, simplifying the conversion from VC to OCT.

In order to make our experiments replicable, we verified that these reductions are deterministic by performing multiple rounds of preprocessing on different machines and checking that the resulting graphs were isomorphic, if small enough to be feasible, and had matching degree, triangle, and number of cliques sequences using the NetworkX `could_be_isomorphic` method otherwise. To verify that these reductions are safe, we saved and verified a certificate (the odd cycle transversal) from each run of a solver that returned a feasible solution.

See the **Reductions** section of REPLICABILITY.md in our repository for information on how to run our scripts for applying these reduction routines.

A.3 Heuristics

We implemented the heuristic ensemble in Modern C++14. Given a graph file and a timeout, the ensemble will run greedy independent set (MinDeg), Luby’s Algorithm (Luby), DFS 2-coloring (DFS), and BFS 2-coloring (BFS) in a round-robin fashion until the time limit is reached, returning the single best solution found by any heuristic. See [Goodrich et al. 2018b] for more on MinDeg, [Luby 1986] for more on Luby, and [Wernicke 2003] for more on DFS.

See the **Utilities/Heuristics Solver** section of README.md in our repository for information on how to run the heuristic ensemble solver.

A.4 Hüffner Improvements

We implemented our improvements to Hüffner’s implementation [Hüffner 2006] in Modern C++14, and rewrote the original solver to compile in C11. By default, the `enum2col` solver is run, with the preprocessing level p specified by the user: The default algorithm ($p = 0$), the default algorithm with a heuristic bipartite subgraph starting the ordering ($p = 1$), and the default algorithm with a heuristic bipartite subgraph starting the ordering and the remaining vertices sorted such edges are introduced as quickly as possible ($p = 2$).

See the **Utilities/Iterative Compression Solver** section of `README.md` in our repository for information on how to download, install, and run this improved iterative compression solver.

B FRUSTRATED CLUSTER LOOP (FCL) DATA

Table 6. Base clique sizes used to generate frustrated cluster loop (FCL) graphs appropriate for four types of quantum hardware. For each hardware type, the size of the base clique is between the size of the hardware’s minimum clique-embedding and minimum biclique-embedding (inclusive).

Hardware	Min Clique-Embedding	Min Biclique-Embedding	FCL Base Clique Sizes
D-Wave 2000Q	64	128	64, 80, 96, 112, 128
D-Wave 8000Q	128	256	128, 144, 160, 176, 192, 208, 224, 240, 256
Pegasus-6	62	104	62, 69, 76, 83, 90, 97, 104
Pegasus-12	134	248	134, 153, 172, 191, 210, 229, 248

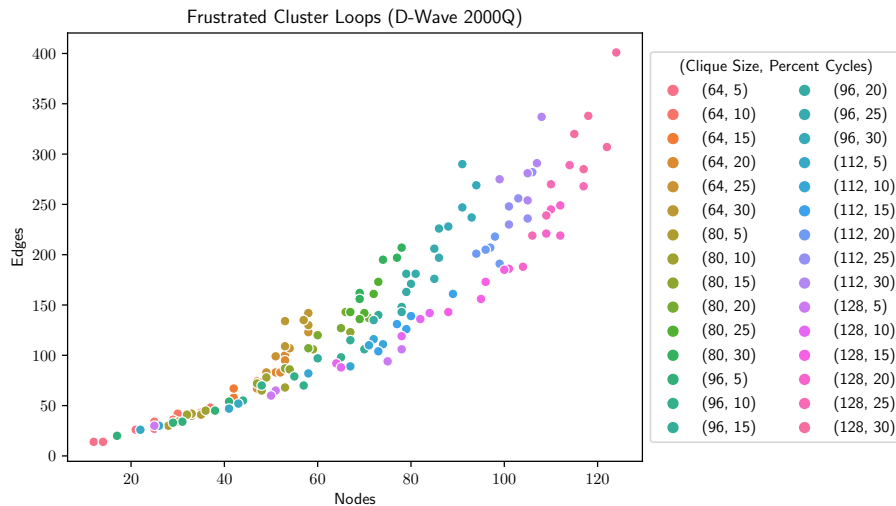


Fig. 3. Instance sizes of frustrated cluster loop (FCL) graphs generated to be appropriate for the D-Wave 2000Q hardware. This hardware can embed a 64-clique and a 128-biclique, so we generated the FCLs from underlying cliques of size $64 \leq n \leq 128$ and varied the number of cycles from 5-30% of the size of the clique. This ensures a corpus of FCLs with size $n \leq 128$, which is the problem space where OCT-embedding methods would be used.

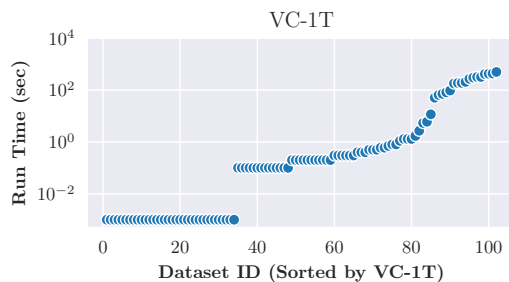


Fig. 4. Run times (log scale) of all quantum datasets when sorted in order of fastest to slowest when solved with the OCT → VC → ILP formulation and one thread (VC-1T).

C EXTENDED RESULTS

C.1 ILP Solver Comparison

As noted in the introduction, previous work [Akiba and Iwata 2016; Hüffner 2009] has conflicting reports on the effectiveness of INTEGER LINEAR PROGRAMMING (ILP) solvers. In this section we identify the best configuration for solving OCT with ILP by using CPLEX with either a formulation from OCT → ILP or OCT → VC → ILP, and evaluate the impact of one thread vs. four. It is well known that GLPK is not competitive with CPLEX, and the 4MB RAM limitations mentioned in [Hüffner 2009] are irrelevant given modern resources, therefore we do not consider these factors.

We find that using the OCT → VC → ILP formulation alone beats the alternative formulation, and that multithreading with this formulation can result in superlinear speedups. Figure 4 visualizes run times for all quantum datasets when sorted in order of fastest to solve with our canonical configuration, the OCT → VC → ILP formulation with one thread. We find that in general (Figure 5), increasing to four threads is worthwhile and can result in a superlinear speedup; we observed speedups over 10× for only a 4× increase in cores. Finally, we observe that the direct OCT → ILP formulation severely impacts CPLEX for the worse, regardless of threads used (Figure 6).

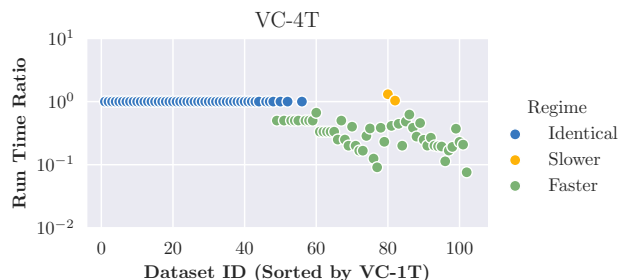


Fig. 5. The run time ratio (log scale) of a 4-threaded solver vs. a single-threaded solver using the OCT → VC → ILP formulation. Easier instances have identical solve times, and all but two of the harder instances benefit from the thread increase.

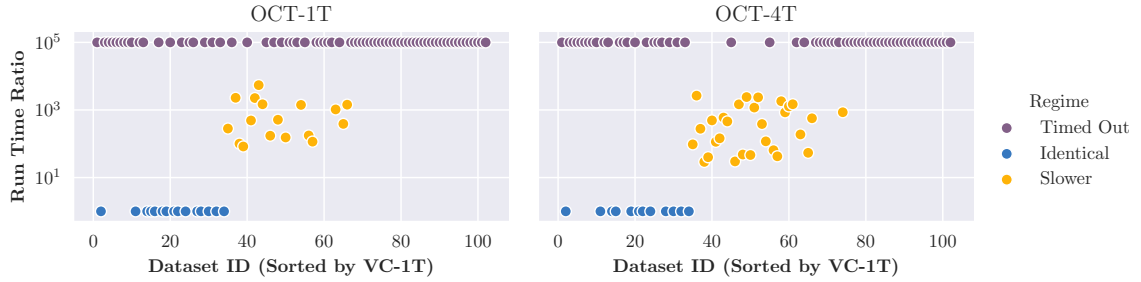


Fig. 6. The run time ratio (log scale) of the single- and four-threaded solvers using the OCT \rightarrow ILP formulation compared to the single-threaded OCT \rightarrow VC \rightarrow ILP formulation (VC-1T). The majority of instances time out at 10 minutes, and no instance is solved faster than with VC-1T.

C.2 Iterative Compression Heuristic Evaluation

We implement our heuristic improvements in a version of Höffner’s code improved for simplicity and compiler compatibility. Recall the preprocessing parameter p defined in Appendix A.4. To evaluate these preprocessing options, we selected a subset of the data with a mixture of easy and difficult problems. We then ran all three levels using 50 random seeds on each instance for each of four timeouts $\{0.01, 0.1, 1, 10\}$, and report mean, standard deviation, and quintiles of the OCT sizes found. Table 7 depicts these results. We find that $p = 1$ always dominates $p = 0$, especially in max and standard deviation, suggesting that certain orderings (avoided with $p = 1$) are significantly disadvantageous for iterative compression. Second, we find that $p = 2$ tends to help on larger timeouts, where the run time cost of computing this ordering disappears. Both observations can be seen in Table 7, where aa-41 and aa-42 benefit slightly from $p = 2$, but gka-2 and gka-3 do not.

C.3 Additional Tables

		OCT Size						
Dataset	p	Mean	S.D.	Min	25%	50%	75%	Max
Timeout: 0.01 (s)								
aa-43	0	21.4	3.0	18	19	21	23	29
	1	18.9	0.7	18	18	19	19	20
	2	19.5	0.6	18	19	20	20	20
aa-45	0	29.6	4.2	22	27	30	32	41
	1	21.8	0.9	20	21	22	22	24
	2	22.7	0.7	21	22	23	23	24
gka-1	0	9.0	0.0	9	9	9	9	9
	1	9.0	0.0	9	9	9	9	9
	2	9.0	0.0	9	9	9	9	9
Timeout: 0.1 (s)								
aa-29	0	35.9	16.2	21	23	32	39	97
	1	22.2	1.3	21	21	22	23	26
	2	23.9	1.7	21	23	24	25	28
Timeout: 1 (s)								
aa-42	0	51.8	13.4	33	42	49	59	85
	1	31.0	1.2	30	30	31	32	35
	2	31.9	0.3	31	32	32	32	32
gka-2	0	16.8	0.9	16	16	17	17	19
	1	16.0	0.0	16	16	16	16	16
	2	16.0	0.0	16	16	16	16	16
Timeout: 10 (s)								
aa-32	0	31.6	2.4	30	30	30	32	38
	1	30.8	0.9	30	30	31	31	33
	2	30.8	0.4	30	31	31	31	31
aa-41	0	67.0	14.4	48	55	64	75	110
	1	41.4	1.2	40	40	41	42	44
	2	41.2	0.7	40	41	41	41	43
gka-24	0	47.1	1.6	44	46	47	48	50
	1	37.9	0.3	37	38	38	38	38
	2	37.9	0.3	37	38	38	38	38
gka-25	0	56.2	2.6	49	55	56	58	62
	1	44.0	0.0	44	44	44	44	44
	2	44.0	0.0	44	44	44	44	44
gka-26	0	57.0	2.3	52	55	57	58	62
	1	43.8	0.4	43	44	44	44	44
	2	43.8	0.4	43	44	44	44	44
gka-27	0	72.3	1.7	68	71	72	74	75
	1	63.0	0.1	62	63	63	63	63
	2	63.0	0.0	63	63	63	63	63
gka-28	0	78.0	1.2	75	77	78	79	80
	1	72.0	0.2	71	72	72	72	73
	2	72.0	0.2	72	72	72	72	73
gka-29	0	82.4	0.8	81	82	82	83	84
	1	77.0	0.0	77	77	77	77	77
	2	77.0	0.0	77	77	77	77	77
gka-3	0	25.2	1.6	23	24	25	26	29
	1	23.3	0.5	23	23	23	24	24
	2	23.4	0.5	23	23	23	24	24

Table 7. Heuristic solution sizes for select datasets at the three levels of preprocessing ($p \in \{0, 1, 2\}$) for Improved Hüffner. The timeout level on each dataset was taken to be the maximum time in $\{0.01, 0.1, 1, 10\}$ less than the time Hüffner at $p = 0$ took to find an exact solution. Mean, standard deviation, and quintiles are computed over 50 samples per timeout, dataset, and preprocessing level.

Dataset	Timeout: OPT'	0.01(s)			0.1(s)			1(s)			10(s)		
		HE	IC	ILP	HE	IC	ILP	HE	IC	ILP	HE	IC	ILP
Wernicke-Hüffner Afro-American Graphs													
aa-10	6	7	6	8	6	6	6	6	6	6	6	6	6
aa-11	11	12	11	15	12	11	13	11	11	11	11	11	11
aa-13	12	15	12	22	15	12	12	14	12	12	13	12	12
aa-14	19	21	19	35	19	19	27	19	19	19	19	19	19
aa-15	6	8	6	12	6	6	6	6	6	6	6	6	6
aa-16	0	0	0	0	0	0	0	0	0	0	0	0	0
aa-17	25	28	28	41	28	27	34	26	27	25	26	25	25
aa-18	14	18	14	21	17	14	14	14	14	14	14	14	14
aa-19	19	22	22	38	21	21	20	21	19	19	21	19	19
aa-20	19	23	24	129	22	20	25	22	20	19	22	20	19
aa-21	0	0	0	0	0	0	0	0	0	0	0	0	0
aa-22	16	17	17	37	17	16	16	17	16	16	17	16	16
aa-23	18	21	21	35	21	18	19	19	18	18	19	18	18
aa-24	21	25	27	150	25	24	46	24	21	21	24	21	21
aa-25	0	0	0	0	0	0	0	0	0	0	0	0	0
aa-26	12	13	12	14	12	12	12	12	12	12	12	12	12
aa-27	11	14	11	13	14	11	11	13	11	11	12	11	11
aa-28	27	33	32	106	31	29	32	30	27	27	30	28	27
aa-29	21	26	26	169	22	24	23	22	21	21	22	21	21
aa-30	4	4	4	4	4	4	4	4	4	4	4	4	4
aa-31	0	0	0	0	0	0	0	0	0	0	0	0	0
aa-32	30	39	35	47	32	35	37	32	33	30	32	31	30
aa-33	4	4	4	31	4	4	4	4	4	4	4	4	4
aa-34	13	16	13	27	13	13	13	13	13	13	13	13	13
aa-35	10	10	10	10	10	10	10	10	10	10	10	10	10
aa-36	7	7	7	18	7	7	7	7	7	7	7	7	7
aa-37	4	5	4	7	4	4	4	4	4	4	4	4	4
aa-38	26	33	31	102	31	27	35	31	26	26	31	26	26
aa-39	23	28	27	40	26	26	26	24	25	23	24	23	23
aa-40	22	25	28	33	22	23	28	22	22	22	22	22	22
aa-41	40	50	46	172	48	45	60	46	45	40	46	41	40
aa-42	30	36	35	160	36	33	43	34	32	30	34	30	30
aa-43	18	19	19	20	19	19	18	19	19	18	19	19	18
aa-44	10	10	10	15	10	10	12	10	10	10	10	10	10
aa-45	20	22	22	20	21	22	20	21	20	20	21	20	20
aa-46	13	18	13	37	16	13	13	14	13	13	14	13	13
aa-47	13	14	13	15	14	13	13	13	13	13	13	13	13
aa-48	17	19	18	21	17	17	17	17	17	17	17	17	17
aa-49	0	0	0	0	0	0	0	0	0	0	0	0	0
aa-50	18	21	19	27	21	18	19	20	18	18	19	18	18
aa-51	11	13	11	16	11	11	11	11	11	11	11	11	11
aa-52	12	13	12	15	12	12	12	12	12	12	12	12	12
aa-53	12	15	12	18	14	12	13	14	12	12	13	12	12
aa-54	12	14	12	21	14	12	14	13	12	12	12	12	12
Wernicke-Hüffner Japanese Graphs													
j-10	3	3	3	3	3	3	3	3	3	3	3	3	3
j-11	5	5	5	5	5	5	5	5	5	5	5	5	5
j-13	4	4	4	4	4	4	4	4	4	4	4	4	4
j-14	3	3	3	3	3	3	3	3	3	3	3	3	3
j-15	0	0	0	0	0	0	0	0	0	0	0	0	0
j-16	0	0	0	0	0	0	0	0	0	0	0	0	0
j-17	10	10	10	16	10	10	10	10	10	10	10	10	10
j-18	9	10	10	12	10	10	9	9	9	9	9	9	9
j-19	3	3	3	3	3	3	3	3	3	3	3	3	3
j-20	0	0	0	0	0	0	0	0	0	0	0	0	0
j-21	2	2	2	2	2	2	2	2	2	2	2	2	2
j-22	9	9	9	9	9	9	9	9	9	9	9	9	9
j-23	19	19	19	19	19	19	19	19	19	19	19	19	19
j-24	3	3	3	3	3	3	3	3	3	3	3	3	3
j-25	0	0	0	0	0	0	0	0	0	0	0	0	0
j-26	6	6	6	7	6	6	6	6	6	6	6	6	6
j-28	13	13	16	16	13	13	13	13	13	13	13	13	13

Table 8. Heuristic solution sizes after 0.01, 0.1, 1, and 10 seconds for the heuristic ensemble (HE), iterative compression IC, and CPLEX (ILP) when run on WH datasets. Highlighting indicates instances where the solver found an exact solution before the provided time limit.

Dataset	0.01(s)			0.1(s)			1(s)			10(s)			
	OPT	HE	IC	ILP	HE	IC	ILP	HE	IC	ILP	HE	IC	ILP
Beasley 50-Vertex Graphs													
b-50-1	11	12	11	15	11	11	12	11	<i>11</i>	<i>11</i>	11	<i>11</i>	<i>11</i>
b-50-2	11	12	11	13	12	<i>11</i>	<i>11</i>	11	<i>11</i>	<i>11</i>	11	<i>11</i>	<i>11</i>
b-50-3	14	15	15	16	14	14	14	14	<i>14</i>	<i>14</i>	14	<i>14</i>	<i>14</i>
b-50-4	11	12	12	14	11	<i>11</i>	11	11	<i>11</i>	<i>11</i>	11	<i>11</i>	<i>11</i>
b-50-5	13	13	13	16	13	13	15	13	<i>13</i>	<i>13</i>	13	<i>13</i>	<i>13</i>
b-50-6	9	9	<i>9</i>	14	9	<i>9</i>	9	9	<i>9</i>	<i>9</i>	9	<i>9</i>	<i>9</i>
b-50-7	9	10	<i>9</i>	12	9	<i>9</i>	<i>9</i>	9	<i>9</i>	<i>9</i>	9	<i>9</i>	<i>9</i>
b-50-8	14	15	15	20	15	15	17	15	<i>14</i>	<i>14</i>	14	<i>14</i>	<i>14</i>
b-50-9	12	13	12	16	13	12	12	13	<i>12</i>	<i>12</i>	12	<i>12</i>	<i>12</i>
b-50-10	11	12	11	13	12	<i>11</i>	11	11	<i>11</i>	<i>11</i>	11	<i>11</i>	<i>11</i>
Beasley 100-Vertex Graphs													
b-100-1	41	43	44	46	43	44	46	43	43	43	43	43	42
b-100-2	42	44	44	47	43	44	47	43	43	43	43	43	42
b-100-3	42	46	45	49	45	45	49	44	44	46	44	44	42
b-100-4	41	43	45	45	42	42	45	42	42	42	42	42	42
b-100-5	42	45	44	47	44	44	47	43	43	45	42	43	43
b-100-6	43	45	46	48	45	45	48	45	45	45	45	45	44
b-100-7	42	45	45	47	44	44	47	44	44	43	44	44	42
b-100-8	43	47	46	48	45	45	48	45	45	47	45	45	43
b-100-9	44	46	47	49	45	45	49	45	45	46	45	45	44
b-100-10	44	46	48	50	45	46	50	45	45	46	45	45	45
GKA Graphs													
gka-1	9	9	<i>9</i>	12	9	<i>9</i>	<i>9</i>	9	<i>9</i>	<i>9</i>	9	<i>9</i>	<i>9</i>
gka-2	16	16	16	19	16	16	17	16	16	<i>16</i>	16	<i>16</i>	<i>16</i>
gka-3	23	24	24	24	24	24	24	24	23	<i>23</i>	23	<i>23</i>	<i>23</i>
gka-4	28	31	31	33	31	30	33	30	30	28	30	30	<i>28</i>
gka-5	22	22	22	23	22	22	23	22	22	<i>22</i>	22	<i>22</i>	<i>22</i>
gka-6	16	16	16	<i>16</i>	16	<i>16</i>	<i>16</i>	16	<i>16</i>	<i>16</i>	16	<i>16</i>	<i>16</i>
gka-7	18	18	<i>18</i>	<i>18</i>	18	<i>18</i>	<i>18</i>	18	<i>18</i>	<i>18</i>	18	<i>18</i>	<i>18</i>
gka-8	28	34	33	33	33	33	33	31	32	28	31	32	<i>28</i>
gka-9	2	2	<i>2</i>	<i>2</i>	2	<i>2</i>	<i>2</i>	2	<i>2</i>	<i>2</i>	2	<i>2</i>	<i>2</i>
gka-10	8	8	<i>8</i>	<i>8</i>	8	<i>8</i>	<i>8</i>	8	<i>8</i>	<i>8</i>	8	<i>8</i>	<i>8</i>
gka-11	10	10	<i>10</i>	<i>10</i>	10	<i>10</i>	<i>10</i>	10	<i>10</i>	<i>10</i>	10	<i>10</i>	<i>10</i>
gka-12	20	20	<i>20</i>	<i>20</i>	20	<i>20</i>	<i>20</i>	20	<i>20</i>	<i>20</i>	20	<i>20</i>	<i>20</i>
gka-13	16	16	<i>16</i>	<i>16</i>	16	<i>16</i>	<i>16</i>	16	<i>16</i>	<i>16</i>	16	<i>16</i>	<i>16</i>
gka-14	22	22	<i>22</i>	<i>22</i>	22	<i>22</i>	<i>22</i>	22	<i>22</i>	<i>22</i>	22	<i>22</i>	<i>22</i>
gka-15	0	0	<i>0</i>	<i>0</i>	0	<i>0</i>	<i>0</i>	0	<i>0</i>	<i>0</i>	0	<i>0</i>	<i>0</i>
gka-16	0	0	<i>0</i>	<i>0</i>	0	<i>0</i>	<i>0</i>	0	<i>0</i>	<i>0</i>	0	<i>0</i>	<i>0</i>
gka-17	0	0	<i>0</i>	<i>0</i>	0	<i>0</i>	<i>0</i>	0	<i>0</i>	<i>0</i>	0	<i>0</i>	<i>0</i>
gka-18	2	2	<i>2</i>	<i>2</i>	2	<i>2</i>	<i>2</i>	2	<i>2</i>	<i>2</i>	2	<i>2</i>	<i>2</i>
gka-19	31	31	31	32	31	<i>31</i>	<i>31</i>	31	<i>31</i>	<i>31</i>	31	<i>31</i>	<i>31</i>
gka-20	39	39	39	40	39	39	39	39	<i>39</i>	<i>39</i>	39	<i>39</i>	<i>39</i>
gka-21	40	41	42	41	41	42	41	41	41	<i>40</i>	40	41	<i>40</i>
gka-22	43	46	46	49	44	46	46	44	46	43	43	45	<i>43</i>
gka-23	46	48	48	52	48	48	51	47	47	47	46	46	46
gka-24	37	39	38	44	38	38	43	38	38	39	37	38	37
gka-25	42	45	46	47	44	44	47	44	44	45	44	44	43
gka-26	43	44	44	50	44	44	50	44	44	43	44	44	43
gka-27	62	65	64	75	64	63	65	63	63	63	63	63	63
gka-28	70	73	73	94	72	72	74	72	72	71	72	72	71
gka-29	77	77	77	95	77	77	80	77	77	79	77	77	78
gka-30	82	83	84	96	83	83	85	83	83	83	83	83	82
gka-31	85	86	87	95	86	87	88	86	86	87	86	86	85
gka-32	88	89	89	97	89	89	90	89	89	89	88	88	88
gka-33	90	91	91	98	91	90	98	90	90	90	90	<i>90</i>	<i>90</i>
gka-34	92	93	93	98	93	92	98	93	<i>92</i>	<i>92</i>	92	<i>92</i>	<i>92</i>
gka-35	0	0	<i>0</i>	<i>0</i>	0	<i>0</i>	<i>0</i>	0	<i>0</i>	<i>0</i>	0	<i>0</i>	<i>0</i>

Table 9. Heuristic solution sizes after 0.01, 0.1, 1, and 10 seconds for the heuristic ensemble (HE), iterative compression IC, and CPLEX (ILP) when run on Beasley and GKA datasets. Highlighting indicates instances where the solver found an exact solution before the provided time limit.